Trends and Spatiotemporal Patterns of Meteorological Drought Incidence in North Wollo, Northeastern Highlands of Ethiopia

Simachew Bantigegn Wassie (simyebb@gmail.com)
Bahir Dar University https://orcid.org/0000-0003-1687-0628
Daniel Ayalew Mengistu
Bahir Dar University
Arega Bazezew Birlie
Bahir Dar University

Research

Keywords: CHIRPS rainfall, Z-Score index, Land Surface Temperature, North Wollo, Ethiopia

Posted Date: October 25th, 2021

DOI: https://doi.org/10.21203/rs.3.rs-977525/v1

Trends and Spatiotemporal Patterns of Meteorological Drought Incidence in North Wollo, Northeastern Highlands of Ethiopia

Simachew Bantigegn Wassie[1], Daniel Ayalew Mengistu[2] and Arega Bazezew Birlie[3]

1. Department of Geography and Environmental Studies, Bahir Dar University, e-mail simyebb@gmail.com P.O. Box 79, Bahir Dar, Ethiopia
2. Department of Geography and Environmental Studies, Bahir Dar University, e-mail dan952002@gmail.com P.O. Box 79, Bahir Dar, Ethiopia
3. Department of Geography and Environmental Studies, Bahir Dar University, e-mail aregaberle@gmail.com P.O. Box 79, Bahir Dar, Ethiopia

Corresponding Author

Simachew Bantigegn Wassie
Department of Geography and Environmental Studies, Bahir Dar University, e-mail simyebb@gmail.com P.O. Box 79, Bahir Dar, Ethiopia

Trends and Spatiotemporal Patterns of Meteorological Drought Incidence in North Wollo, Northeastern Highlands of Ethiopia

Abstract

The study was aimed to detect and characterize meteorological drought risk areas using remote sensing data in North Wollo, Ethiopia. Climate Hazards Group InfraRed Precipitation with Stations (CHIRPS) rainfall estimate was used to compute Z-Score Index (ZSI) and depict droughts during the *meher* season (2000 – 2019). MOD13Q1 from Moderate Resolution Imaging Spectroradiometer (MODIS) image datasets was also used to generate Land Surface Temperature (LST) to investigate its association and trend with ZSI and the precipitation. To analyze the seasonal and annual rainfall trend, Mann-Kendal (MK) test was applied, and Sen's slope estimator was used to fix the magnitude of change. The MK test result revealed that an increasing trend of total annual rainfall (1.2 – 10.7 mm year^{-1}) has been observed in many districts, while the *kiremt* season showed a decreasing trend (-0.43 to -3.85 mm year^{-1}). However, the *belg* (0.05 – 0.23 mm), and *bega* (0.54 – 2.80 mm) seasons revealed a slightly increasing trend in some districts. The ZSI value revealed that 2002, 2004, 2009, 2011, 2014, 2015, and 2019 were characterized by a rainfall deficit resulting in droughts. Though the spatial extent and intensity level varies, there has been drought incidence in the area each year. However, 2009 and 2015 were the driest years with Z-score intensity of -2.01 to -2.84. Based on the regression and correlation result, ZSI has positive significant relationship (r = 0.93 – 0.99) with precipitation, and negative (r = -0.1 to -0.52) with LST. Thus, ZSI showed a significant increasing trend with rising precipitation and decreasing with LST. In the last 20 years, each district of the area encountered a rainfall deficit repeatedly (15 – 18 times), so that the area is categorized as an extremely high meteorological drought risk zone. Such spatiotemporal meteorological drought risk events have an imminent threat to the rainfed agricultural activities imposing immense influence on agro-based livelihoods of the local community. Therefore, it demands continuous drought monitoring and application of effective early warning systems.

Key Words CHIRPS rainfall; Z-Score index; Land Surface Temperature; North Wollo; Ethiopia

1. Introduction

Drought is the most complex and highly damaging natural hazard (Mahyou et al. 2010; Mera 2018) occurring in all climate regimes, and almost all parts of the world (Kiem et al. 2016). It is expected to get worsen in the future with predicted climate change (Eze et al. 2020). The frequency, duration, severity levels, and the aerial extent of drought-affected regions are, therefore, projected to increase having various impacts on the society, country economy, and the environment at large (Yuan et al. 2017; Guo et al. 2018).

Many countries of the world are vulnerable to the consequent impacts of droughts (Trnka et al. 2018). Most of the countries in Africa are regularly affected by severe droughts, which sometimes last for years causing huge socio-economic and environmental costs (Dutra et al. 2013; Lyon 2014). In this regard, Sub-Saharan Africa (SSA) region is widely considered to be the most drought-prone in the continent. This is evidenced that over 363 million people of

the region were affected by drought incidences between 1980 and 2014. Within this period, Ethiopia had the highest losses of all the countries in the region with 61 million people affected (Adhikari et al. 2015; FAO 2015).

In Ethiopia, drought has become a recurrent phenomenon imposing wide-ranging impacts on agriculture, ecosystem sustainability, water, forest resources, energy supply, transportation, recreation, food availability, and other human activities (Kogan et al. 2019; Wassie 2020). In the period 1950 to 2017, drought occurred 34 times in different parts of Ethiopia, revealing that meteorological and agricultural drought broke out every two years (NMA 2007; Mera 2018). Such situations abruptly increase the vulnerability of the Ethiopian population, disrupts their livelihoods, and subject them to chronic and transitory food insecurity (Ahmadalipour 2017; Mpelasoka et al. 2018). Consequently, it erodes environmental resources that could otherwise have been used for development (Gray and Mueller 2012; Azadi et al. 2018). Generally, drought in Ethiopia had swept almost all regions of the country including those places which were drought-free in the past. However, the northeastern, eastern, southeastern, and rift valley regions are those affected more frequently than the others (Mekonnen and Gokcekus 2020).

Previously, droughts, famines, and epidemics have all frequently occurred in the North Wollo Zone and its environs (Gebre et al. 2017). This was unfavorably exposing the population to starvation and immense destitution. All the districts in the Zone are considered as the most drought-prone and chronically food-insecure areas (Hailu 2013). In this area, about 42% of the farming households' production systems fail to meet their basic demands making them face a hungry season each year (Aragie and Genanu 2017). With such complexities, agricultural productivity in the area may fall below recovery levels, and environmental degradation and deterioration of natural resources may occur to the point that the ecosystem can no longer sustain life. Accordingly, it is necessary to make a concerted effort to detect droughts early to successfully monitor and mitigate their impacts (Gao et al. 2008; Dutta and Kundu 2015; Trnka et al. 2018).

Application of Geographic Information Systems (GIS) and remote sensing techniques in the detection, assessment, and monitoring of droughts are becoming important to deliver up-to-date information on a variety of spatial and temporal scales (Singh et al. 2017; Baniya et al. 2019). It allows for cost-effective and spatially explicit data collection and helps to effectively monitor droughts in a larger area (Gaikwad et al. 2015; Zhang et al. 2016). Hence, such methods are important to produce more precise, flexible, and reliable outputs (Bayissa et al. 2018). Traditionally, however, meteorological drought indicators are computed based on direct measurement of climatic variables like rainfall, evapotranspiration, and temperature (Dai 2011).

Several indicators (indices) have been developed to determine how far precipitation has varied from historically established norms over a certain period. The majority of these indices are driven by precipitation variations (WMO and GWP 2016). Some of the widely applied meteorological drought indices include the Palmer Drought Severity Index (PDSI) (Palmer 1965), Percent of Normal (PN), Deciles (Gibbs and Maher 1967), Rainfall Anomaly Index (RAI) (Van Rooy 1965), Drought Area Index (DAI) (Bhalme and Mooley 1980), and Standardized Precipitation Index (SPI) (McKee et al. 1993).

Each model has its strengths and weaknesses (Zargar et al. 2011; Dai 2011). For instance, PDSI is advantageous since it uses complete water balance models to account for the effect of both precipitation and temperature (Dai 2011). However, it requires a lot of data and does not operate well in mountainous places where rainfall is intense (Ellis et al. 2010). It is also limited in the identification of drought at a shorter time scale and shows a problem of calibration and spatial compatibility (Vicente-Serrano et al. 2010). Indices like SPI are useful for any location based on a series of accumulated precipitation for a fixed time scale (McKee et al. 1993). It is also preferred to make drought analyses for a range of all types (Morid et al. 2006; Mpelasoka et al. 2008). In contrast, indices like DAI do not apply to multiple timescales and are specifically designed to be applicable only for the Indian monsoon season (Dai 2011; WMO and GWP 2016). RAI also requires a serially complete dataset without missing values (Tilahun 2006).

The present study considered Z-score Index (ZSI) (Verdin and Klaver 2002) which was developed by using CHIRPS precipitation estimate. It has been applied in many drought studies due to its ease of measurement, and effectiveness (Morid et al. 2006; Dogan et al. 2012; Jain et al. 2015). Several researchers have also praised it for being as successful as the SPI, and being able to measure several time steps (Wu et al. 2001; Patel et al. 2007; Li et al. 2019). Furthermore, it can also accommodate data series with missing values. As a limitation, it doesn't accurately reflect shorter time scales (Jain et al. 2015; WMO and GWP 2016).

Except for a few recent efforts, identifying agricultural drought risk in the study area has largely relied on mechanical analysis of ground-based temperature and rainfall data over a short time frame. It is extremely difficult to collect sufficient spatial and temporal data using this method alone, especially in locations like North Wollo, which are characterized by rugged topography, variable rainfall, and limited accessibility. Drought analysis based on data acquired in such conditions may fail to better capture historic drought patterns (Dogan et al. 2012). To this end, the objective of this study was to identify meteorological drought risk areas and characterize it using remote sensing

data, and other thematic information. Thus, the findings could be useful in facilitating effective drought monitoring, early warning, and mitigation efforts in the study area and Ethiopia at large.

2. Materials and Methods

2.1 Study Area

The study was carried out in the North Wollo Zone which is part of the northeast Ethiopian highlands. It is situated between 11^0N and 12^0N latitude, and 39^0E and 40^0E longitude. The zone has an estimated area of 12,179.6 km^2, which covers about 20% of the total area of the ANRS (Gebre et al. 2017). It has ten rural districts and four town administrations. The topography of the area includes steep, rugged, mountainous places which are not sustainable for agricultural activities. Its altitude varies from 968 meters in Habru district to 4,258 m.a.s.l at the tip of Mount Abuna Yosef in the Lasta district (Hailu 2013). The majority of the area remains inaccessible due to the lack of all-weather roads. In terms of agro-ecology, Lowland (*Kolla*) from 786-1500, mid-latitude (*Woina-dega*) 1500-2300, Highland (*Dega*) 2300-3200, and *Wurch* from 3200-4258 m.a.s.l covers 38, 34, 21 and 7% of the Zone, respectively (Gebre et al. 2017).

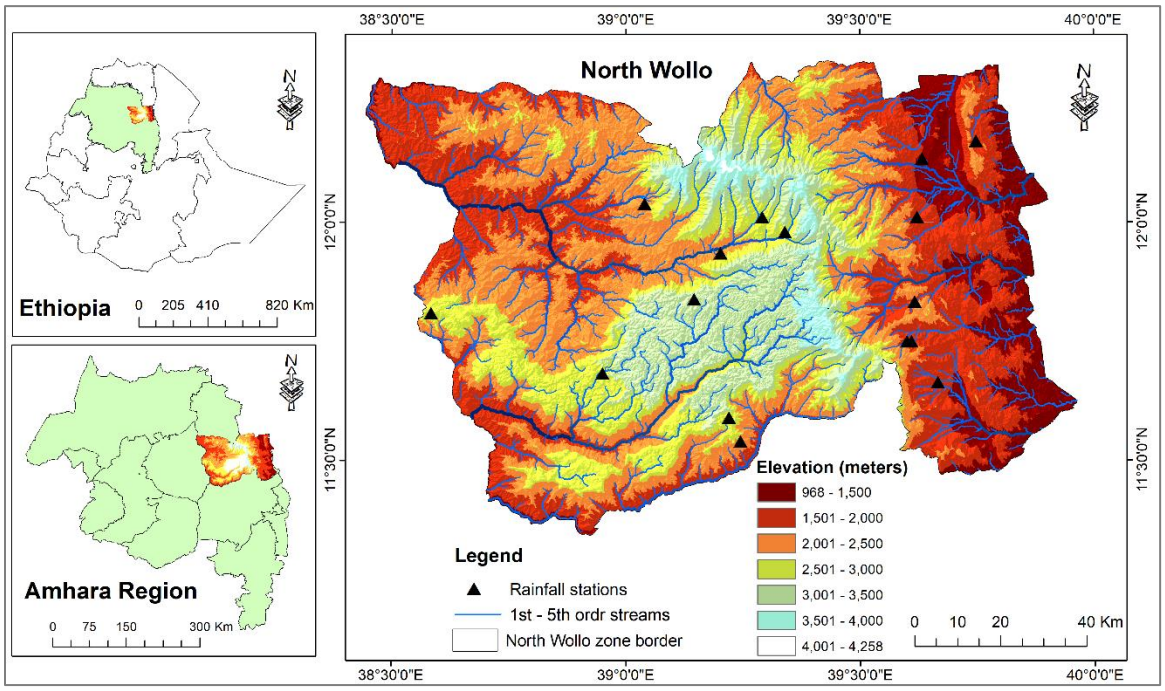

Fig. 1 Map of the study area

In 2017, the zone's overall population was projected to be 1,824,361, with 913,572 males and 910,789 females. From this, more than 85.2% of the Zone's population lives in rural areas (CSA 2013). Based on rainfall data from thirteen meteorological stations in the region (1992 - 2019), the average annual mean maximum temperature ranges

from 20.6°C in some highland parts to 30.4°C in the lowland parts of the area. The annual mean minimum temperature extends from 7.1^0C to 15.4^0C in the cool and warm drier parts of the zone respectively. It also receives a maximum total annual rainfall of 1061.2 mm in the *woina-dega* and (624.8mm) in the drier parts of *Kolla* agro-ecologies (Analysis from NMA data). In most cases, the highland parts of the area rely on *belg* rain for crop production, whereas the *Woina dega* and *Kolla* areas are *Meher* rain-dependent (Aragie and Genanu 2017).

2.2. Data Acquisition

CHIRPS Precipitation Data

Climate Hazards Group InfraRed Precipitation with Stations (CHIRPS) satellite rainfall product was used as a dataset to depict the meteorological drought. It was developed by the US Geological Survey (USGS) and the Climate Hazards Group at the University of California, Santa Barbara (Eshetie and Demisse 2016; Munira et al. 2018). It is a blended product combining data from several sources such as the monthly accumulated climatologically precipitation from CHPClim, the product of the Climate Prediction Center (CPC) and the National Climatic Data Center (NCDC), the TRMM precipitation estimation, quasi-global geostationary thermal infrared (TIR) satellite observations from the National Climate Forecast System version 2 (CFSv2) and, in situ observations of precipitation obtained from national and regional meteorological services. Such data is available from 6-hourly to 3-monthly aggregates in NetCDF, GeoTiff, and Esri BIL formats. Almost all data has a 0.05° × 0.05° spatial resolution. It is available at a spatial dimension for Africa within (1500 × 1600 pixels, 20°W to 55°E and 40°N to 40°S). A detailed description of the product is found in (Funk et al., 2015).

Various studies (Dinku et al. 2018; Gebrechorkos et al. 2018; Munira et al. 2018) evaluated the performance of CHIRPS rainfall estimates with other satellite products over East Africa. As a result, CHIRPS was found to be perceived as more robust in representing the rainfall field, as it is blended with ground measurements. Therefore, CHIRPS is used in this study because of its high accuracy shown in Ethiopia (Funk et al. 2015; Ayehu et al. 2018). In addition, it has a higher spatial resolution (~5.5 km) and covers a longer period (1981 to present) than other products. The CHIRPS data was used to calculate rainfall-based ZSI.

MODIS image datasets

The moderate resolution imaging spectroradiometer (MODIS), a recent successor to the Advanced Very High-Resolution Radiometer (AVHRR) sensor, is a key instrument aboard NASA's Earth-observing system (EOS) with Terra and Aqua spacecraft (Thenkabail et al. 2004). Despite its relatively shorter data record, MODIS outperforms

AVHRR in that it provides observations with higher spatial resolutions (250 m, 500 m, and 1 km), more spectral channels, more accurate geo-location, and improved atmospheric corrections (Ghaleb et al. 2015; Liou and Mulualem 2019). Accordingly, its data products provide a good opportunity for more accurate and higher resolution monitoring of droughts (Cai et al., 2011; Wu et al., 2015). The data was freely accessed from https://earthexplorer.usgs.gov. For this study, a total of 320 (LST) scenes were acquired for the *Kiremt* season (June to September) for the period 2000 to 2019. Such successive images were used to compute LST to see its influence on ZSI and CHIRPS rainfall.

2.3. Validation of CHIRPS rainfall

Before implementing it in specific geographical areas and hydro-climatic conditions, remote sensing data and models for drought monitoring and early warnings must be validated and calibrated (Eshetie and Demisse 2016). In the present study, for the validation of the CHIRPS rainfall estimate, ground-based daily rainfall data were collected from National Meteorology Agency (NMA) on thirteen different stations of the study area within the specified years (2000 – 2019). Rainfall data screening was primarily done in each station through visual inspection. As a result, there exist shortage of long-term continuous database; some input data from the stations used were totally or partly missing. To get continuous data, such missed records were filled by using the interpolation method of the K-Nearest Neighbor Algorithm in R-software.

Table 1 History of the thirteen meteorological stations in North Wollo

Station Name	*Record Length*	*Class*	*Latitude*	*Longitude*	*Elevation (m)*	*Agro-ecology*	*Location (Woreda)*
Lalibela	1992-2019	1	12.039	39.03984	2487	*Woina-dega*	Lasta
Muja	1995-2019	4	12.01077	39.29147	2795	*Dega*	Gidan
Kulmesk	1992-2019	4	11.93544	39.20238	2362	*Woina-dega*	Gidan
Estayish	1999-2019	4	11.83878	39.14589	3295	*Wurich*	Meket
Zobil	1998-2019	3	12.17086	39.74843	1893	*Woina-dega*	Kobo
Kobo	1996-2019	1	12.13333	39.63333	1470	*Kolla*	Kobo
Robit	2001-2019	4	12.0115	39.6221	1629	*Kolla*	Kobo
Weldiya	1992-2019	3	11.83333	39.61667	1897	*Woina-dega*	Gubalafto
Mersa	1992-2019	3	11.66381	39.66605	1578	*Kolla*	Habru
Kone	1996-2019	3	11.68333	38.95	2890	*Dega*	Wadla
Gosh Meda	2000-2019	4	11.54006	39.24476	2261	*Woina-dega*	Delanta
Hara	2006-2019	3	11.75	39.6	1980	*Kolla*	Habru
Debre Zebit	1998-2019	3	11.8094	38.584	2919	*Dega*	Meket

The refined monthly rainfall data were used to validate the CHIRPS monthly rainfall estimate extracted in similar station points with the same timeframe. Thus, among the pair-wise comparison statistics techniques, the

Pearson correlation coefficient (r), Mean error *(ME)*, Mean absolute error (MAE), Root Mean Square Error (*RMSE*), and Bias were applied in the evaluation technique. The detailed description of these indices is found in Toté et al (2015) and many researchers used part or all of such indices in their validation process of CHIRPS rainfall estimates (Bayissa et al. 2017; Gebremicael et al. 2017; Dinku et al. 2018; Camberlin et al. 2019).

The Pearson correlation coefficient (r) measures how well the two variables fit together and how linearly they are related. It measures how well the satellite rainfall product corresponds to the observed rainfall as expressed by the equation below. Here, the value of *r* varies between 0 and 1, in which one indicates the perfect score, and zero for no relationship between the two.

$$\mathbf{r} = \frac{\sum(G-\bar{G})(C-\bar{C})}{\sqrt{\sum(G-\bar{G})^2}\sqrt{\sum(C-\bar{C})^2}} \quad (1)$$

Where, r = the correlation coefficient, G = gauge rainfall measurement, $\bar{G}$ = average gauge rainfall measurement, C = CHIRPS rainfall estimate, $\bar{C}$= average CHIRPS rainfall, and n = number of data pairs.

The *ME* refers to the average of all the errors in a set of measurements (Eq. 2). In the comparison of the observed gauging rainfall and CHIRPS rainfall, a positive value of *ME* indicates an overestimate of the CHIRPS rainfall, whereas a negative value indicates its underestimate; whilst the *ME* value of zero indicates a perfect score or no error.

$$ME = \frac{\sum(C-G)}{n} \quad (2)$$

Where, ME= the mean error, C=CHIRPS rainfall estimate, and G=gauge rainfall measurement, and n= number of data points

The MAE is a measure of errors between two paired observations (satellite rainfall observation and rainfall from gauging stations) which express the same issue. It is the arithmetic average of the absolute errors of data points (Eq. 3). Its value ranges from 0 to positive infinity, where the value approaching zero indicates minimum error between the two measurements.

$$MAE = \frac{\sum|C-G|}{n} \quad (3)$$

Where, MAE= the mean absolute error, C=CHIRPS rainfall estimate, and G=gauge rainfall measurement, and n= number of data points

The RMSE is applied to measure the average magnitude of the estimated errors between the satellite rainfall and the gauged rainfall (Eq. 4). A lower RMSE value means greater central tendencies and small extreme error. The RMSE value of zero shows the perfect score.

$$RMSE = \sqrt{\frac{\sum_{i=1}^{n}(C_i-G_i)^2}{n}} \quad (4)$$

Where, RMSE is the root mean square error, G_i = gauge rainfall measurements, S_i = CHIRPS rainfall estimates, and n= number of data points

On the other hand, the degree to which the mean of satellite rainfall matches the mean of observed rainfall is referred to as bias (Eq. 5). The average satellite rainfall estimate is closer to the cumulative observed rainfall when the bias value is closer to one, whereas the perfect score has a bias value of one.

$$Bias = \frac{\sum C}{\sum G} \quad (5)$$

Where, C = CHIRPS rainfall estimate and G = gauge rainfall measurement

2.4 Data Processing and Analysis

2.4.1 CHIRPS rainfall variability and trend assessment

Coefficient of variation (CV) was employed to detect the nature of the annual and seasonal rainfall variability at each of the selected rainfall stations for the observation period (2000 – 2019). Different studies indicated that the CV is a percentage-based statistical measure of the relative dispersion of data points in a data series around the mean (Achite et al. 2021). It is the measure of the potential seasonal and inter-annual fluctuations in rainfall availability for regions. Increased CV indicates larger seasonal and/or year-to-year fluctuations, and therefore, less predictability in the climate leading to a high risk of extreme events such as droughts. As documented by Hare (2003) and applied by Belay et al. (2021), the degree of rainfall variability is classified as low (CV < 20), moderate (20% < CV > 30%) and high (CV > 30%). The CV was statistically computed using (Eq. 6):

$$CV\ (\%) = \frac{\sigma}{\bar{x}} * 100 \quad (6)$$

Where CV= percent CV for each station, σ= seasonal or annual rainfall standard deviation, $\bar{x}$ =long-term mean value

For trend detection, the most commonly used non-parametric test, Mann-Kendall (MK) test, was employed to investigate the possible trend in annual and seasonal rainfall series in each selected station of the study area. MK test was selected basically because it is more appropriate for the situations of non-normally distributed data, incomplete data, and missing data problems, which frequently occur in hydro-meteorological studies (Gocic and Trajkovic 2013). MK-test helps to determine the presence of statistically significant or non-significant trends of rainfall in the time series without requiring normality or linearity as it is a distribution-free test (Wang et al. 2008; Jain and Kumar 2012). Thus, to evaluate the significance of the trend, the statistic ***S*** was first estimated (Eq. 7).

$$S = \sum_{i=1}^{d-1} \sum_{j=i+1}^{d} sgn(xj - xi)\,; with\ sgn(xj - xi) = \begin{cases} 1\ if\ (xj - xi) > 0 \\ 0\ if\ (xj - xi) = 0 \\ -1\ if\ (xj - xi) < 0 \end{cases} \quad (7)$$

Where x_j & x_i = *the variable values in the years j & j (with j > i), respectively and d= dimension of the series*

If n is less than 9, the absolute value of S is directly compared to MK's hypothesized distribution of S. If *n* is at least 10 the normal approximation test is used. Given independent and randomly ordered values, for the d > 10, the statistic S is distributed following a normal distribution with zero means (Blain 2013; Rahman et al. 2017) and the variance computed as:

$$Var\ (S) = [d(d-1)(2d+5) - \sum_{i=1}^{m} t_i i(i-1)(2i+5)]/18 \quad (8)$$

With t_i = a number of i-fold ties

Finally, the standardized statistics Z_{MK} was calculated (Eq. 8):

$$Z_{MK} = \begin{cases} \frac{S-1}{\sqrt{Var\ (S)}} \ for\ S > 0 \\ 0\ for\ S = 0 \\ \frac{S+1}{\sqrt{Var\ (S)}} \ for\ S < 0 \end{cases} \quad (9)$$

The Z value is used to determine whether a statistically significant trend exists. An upward (downward) trend is indicated by a positive (negative) Z value. When testing if there exist an upward or downward monotone trend (a two-tailed test) at α level of significance, *H0* is rejected if the absolute value of *Z* is greater than $Z_{1-\alpha/2}$. The $Z_{1-\alpha/2}$ is obtained from the standard normal cumulative distribution tables with the tested significance levels of α at 0.001, 0.01, 0.05 or 0.1. XLSTAT 2021 software was used for detecting and estimating variability and time-series trends of monthly seasonal and annual rainfall estimations.

2.4.1. Z-Score Index

Z-score index (ZSI) is also known as a rainfall deficit index or Statistical Z-Score. It is the other form of SPI, a commonly used meteorological DI (Li et al. 2019). ZSI is a rainfall-based index that can able to quantify both dry and wet cycles (Wu et al. 2001; Dogan et al. 2012). Various studies in their comparisons of DIs effectiveness also reported that ZSI responds similarly to the complex SPI and China Z-Index (CZI) (Morid et al. 2006; Salehnia et al. 2017). The computational procedure of the ZSI is also similar to that of SPI. However, the ZSI in the present study was computed using the spatial input data and applied only for the normally distributed probability density functions. It was calculated for the crop growing (*meher*) season in a 4-month time scale of the study period (2000 – 2019) to make it comparable with the agricultural drought indices which will be computed from MODIS data. Several studies (Wu et al. 2001; Morid et al. 2006; Patel et al. 2007; Dogan et al. 2012; Li et al. 2019) commonly computed ZSI in their drought analysis and obtained good results.

As a data source, CHIRPS Monthly rainfall estimate (CHIRPS v.2) was obtained from the https://data.chc.ucsb.edu/products/CHIRPS-2.0/africa_monthly/ for about 20 years (2000 – 2019). The raster data for the required months and years was clipped to the study area, and the necessary computations were made accordingly using Arc GIS 10.4.1 software. Hence, ZSI reveals how many standard deviations a rainfall value deviates from the long-term mean. The classification for the drought category is indicated in Table 2. The equation below summarizes the calculation procedures of the ZSI.

$$ZSI = \frac{P_i - \bar{P}}{\sigma} \quad (10)$$

Where, Pi = precipitation in a specific month, $\bar{P}$ = long-term mean monthly precipitation (the long-term 4 month average of each year), and σ = the standard deviation of the rainfall data over those months in the time series.

Table 2 Drought categories defined for Z-score index values

Z-Score index value	Drought Category
≥ 2.0	Extremely wet
1.5 to 1.99	Very wet
1.0 to 1.49	Moderately wet
0.99 to −0.99	Near normal or Mild drought
−1.0 to −1.49	Moderate drought
−1.5 to −1.99	Severe drought
≤ −2.0	Extreme drought

Source: Li et al. (2019)

Land Surface Temperature (LST)

LST is one of the MODIS global LST / Emissivity products which measures the Earth's surface temperature (Bentoa et al. 2018). The daily Terra-based MOD11A2 LST data was used as a data source for this study. About 320 MOD11A2 LST C6 Terra data product was used to assess the seasonal LST condition of the study area for the study period. The MOD11A2 LST during 8-days period with a spatial resolution of 1km, which was later aggregated to a monthly basis, was used for analysis. The data is normally stored in the Hierarchical Data Format (HDF-EOS) and sinusoidal projection. So, the MODIS conversion tool kit (MCTK) was used to convert the projection from sinusoidal into USGS-84 Zone 37 geo-tiff format using ENVI software. In the meantime, the required LST data were rescaled with 0.02 to obtain the LST value in Kelvin units. Finally, LST values were converted to degrees Celsius (°C) by deducting 273.15 from each grid cell (Sruthi and Aslam 2015).

$$LST = (\partial \times 0.02) - 273.15 \quad (11)$$

Where, LST=land surface temperature in degree Celsius (°C), ∂=row scientific data

2.4.6. Trend, Regression, and Correlation Analysis

To analyze the trend between the anomalies of Precipitation (PPt) and LST, and the ZSI, a simple linear regression model was employed. In the model, anomalies of PPt were considered as the independent variables influencing the dependent variables such as ZSI and LST. On the other hand, the LST anomaly was considered as the other independent variable used to examine its effect on ZSI. To observe how the climate variables (PPt and LST) are related to ZSI in determining drought conditions, Pearson's correlation coefficient matrix was developed. A four-by-four correlation matrix was prepared for the five selected stations (Kobo, Lalibela, Kone, and Estayish) fairly representing four different agro-ecologies. The statistical significance of the trend and correlation coefficient values were also tested using t-test distribution. XLSTAT 2021 software was applied for the entire statistical computation.

2.4.7. Classification of Drought Risk Area

A drought risk map for the study area was produced using a ZSI-based drought frequency map. For the frequency of drought episodes, we used the 20 different drought severity class images generated by the ZSI. Each binary image in each year was reclassified into the Boolean image to represent either drought or non-drought conditions. Afterward, the images of each year were sum-up to get a drought frequency at each pixel level.

Drought probability zones in an area can be classified as high, moderate, or low risk, when drought occurs over 50 percent, 30 to 50 percent, or less than 30 percent of the years, respectively (Gonfa 1996). The frequency map was classed based on this criterion into five levels of drought risk zone: 0-2 for no drought risk; 3-5 low drought risk; 6-10 moderate drought risk; 11-14 high; and 15 and above for very high drought risk zones. Numerous studies such as Gebre et al. (2017), Legesse & Suryabhagavan (2014), and Senamaw et al. (2021) applied such a method to produce maps showing meteorological and/or agricultural drought risk areas in many parts of Ethiopia.

3. Results and Discussion

3.1. Validation results of CHIRPS rainfall estimates

The observed rainfall data from 13 selected gauging stations in the Zone were used to evaluate CHIRPS rainfall. For each station, Pearson correlation, ME, MAE, RMSE, and bias evaluation parameters were considered for both annual and monthly time scales. The findings revealed that a strong correlation was detected between CHIRPS rainfall and observed rainfall in the majority of the stations. On a monthly time scale, the correlation coefficient (r)

ranged from 0.74 (Kobo) to 0.95 (Lalibela), and on the annual time scale, it extended from 0.37 (Zobel) to 0.83 (Lalibela). The correlation was strong for monthly than the annual time steps (Fig. 2a).

Monthly and annual multiplicative bias values were the same in each of the stations. It ranges from 0.89 (Robit) to 1.49 at Gosh Meda. The bias values for most stations were close to one (Fig. 2b). Consequently, overestimation of rainfall (bias > 125%) was detected only on Gosh-Meda (149%) and Hara (126%), but underestimation (bias value < 75%) was not observed at any of the stations. This demonstrates that CHIRPS and the gauged rainfall have a strong agreement in terms of bias values. The ME for annual and monthly time steps was computed to be the same. A positive value of ME was registered in five stations with the lowest at Robit (-7.2 mm) and the highest at Zobel (-0.8 mm) in each Month (Fig. 2c). Excess rainfall was also registered on the remaining eight stations with the highest at Gosh-Meda (24.3 mm/month). The MAE (Fig. 2d) was also computed showing that lower deviation of rainfall value was registered on annual and higher value at the monthly time scales. Although it varies from station to station, the average difference of CHIRPS rainfall estimate from gauging measurements reached 27.2 for monthly and 13.9 mm/month for annual time steps. On the other hand, comparisons of RMSE at annual and monthly time scale again show a minimum value at annual and higher values at the monthly time scales (Fig. 2e). So, it assures that greater central tendency and small extreme error have, relatively, been observed at the annual than the monthly rainfall estimates.

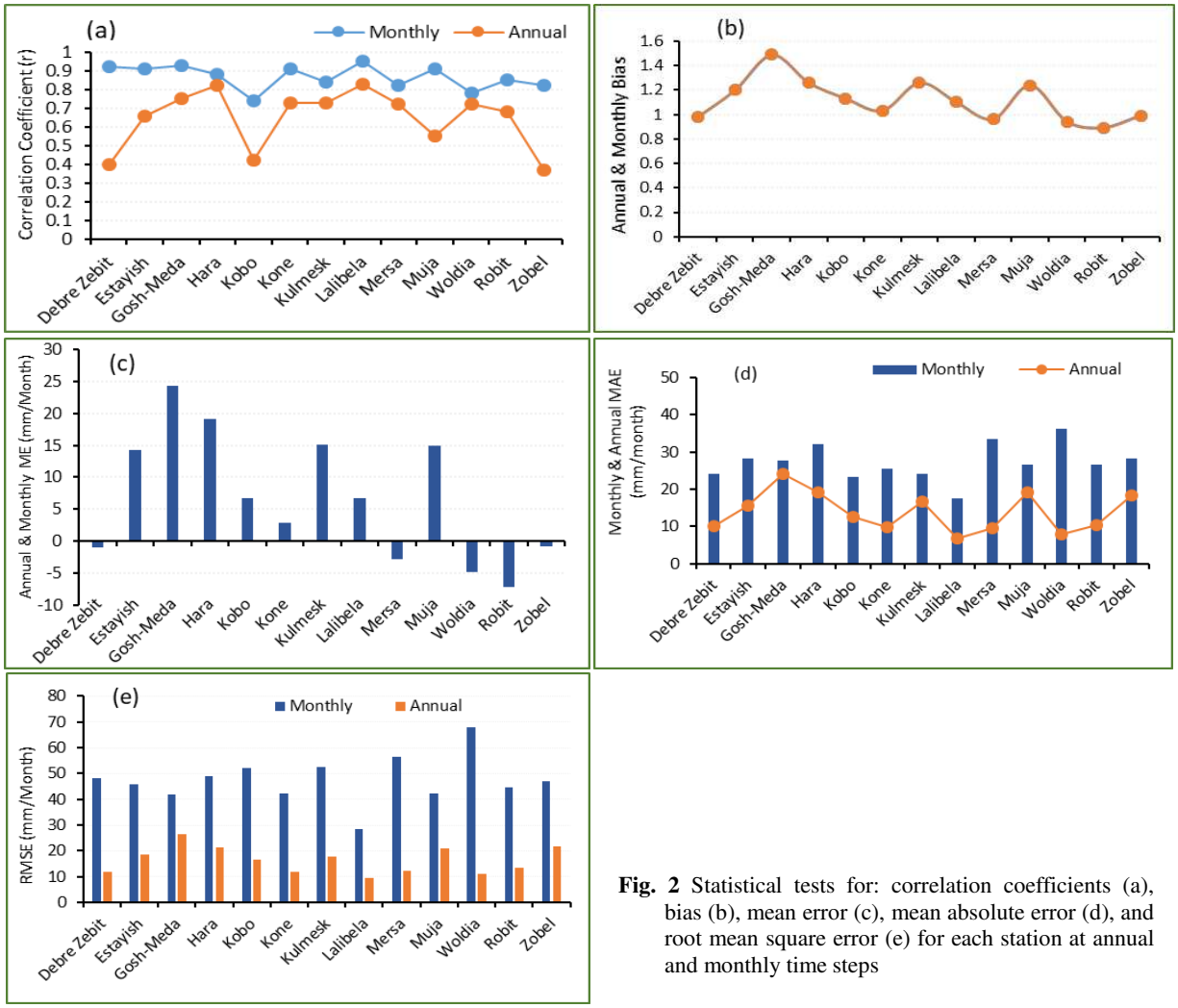

Fig. 2 Statistical tests for: correlation coefficients (a), bias (b), mean error (c), mean absolute error (d), and root mean square error (e) for each station at annual and monthly time steps

Scatter plots were also generated for monthly, and annual time steps using the time series data of the 13 selected stations. The plots were produced by aggregating each of the CHIRPS and observed rainfall data in all the independent stations. As shown in Fig. 3 (a), it is to mean that at 96.2% of the time, a 1mm increase of observed rainfall record in each month was accompanied by a 1.02 mm rise of CHIRPS rainfall in the time series, which is nearly equal. In addition, the coefficient of determination (R^2) values of 0.96, and 0.79 were obtained for the monthly and annual timescales, respectively. This is evident for the good agreement of CHIRPS rainfall estimate with the observed rainfall data. Generally, the results of all statistical tests revealed that CHIRPS monthly rainfall products could potentially be useful in detecting and assessing meteorological and agricultural droughts in data-scarce regions of Ethiopia and the study area in particular.

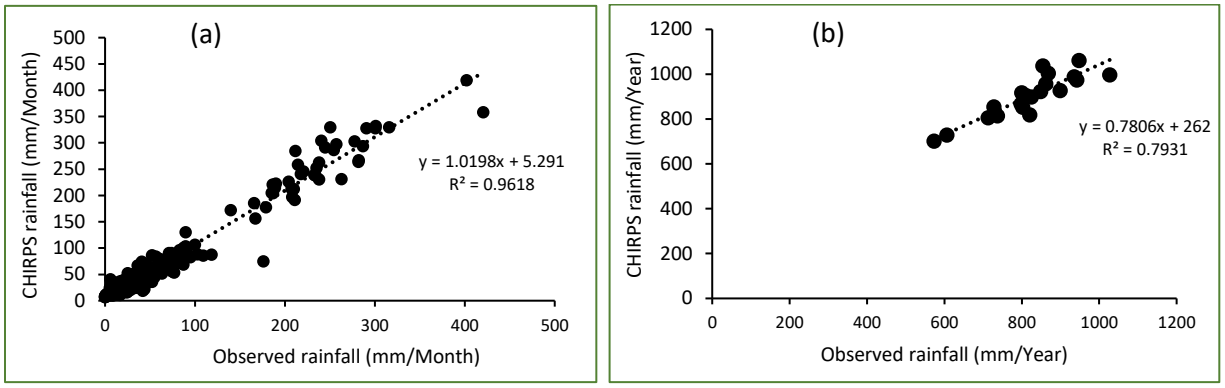

Fig. 3 Scatter plots for CHIRPS and observed rainfall at monthly (a), and annual (b) time scales

3.2. Variability and trend analysis of CHIRPS rainfall

As shown in Table 3, the long-term (2000 – 2019) mean annual rainfall ranges from 708.1 – 1073.0 mm with a standard deviation ranging from 100.8 – 144.8, and a coefficient of variation of 10.8 – 16.0%. The highest mean annual rainfall was registered in Hara station while the lowest was in Zobel station. In the entire study area *Kiremt, Bega* and *Belg* seasons had contributed about 52.7, 14.6, and 32.7% of the total annual rainfall respectively. Similar studies conducted by Mekonen and Berlie (2020) in South Wollo and Ayalew (2012) in Amhara Region concluded that the maximum share of the total annual rainfall is obtained during the *kiremt* season. Many other similar studies conducted across different parts of Ethiopia (Bewket 2009; Gebrehiwot and Veen 2013; Suryabhagavan 2017) firmly indicated that *bega* season contributes the smallest (4 - 15%), *belg* season about (5 - 30%), and *kiremt* season the highest (54–85%) share of the total annual rainfall.

The coefficient of variation (CV) result shows that the CV of the total annual rainfall was found to be smaller than the CV of each season in all the stations. The CV of each season was also variable within a station and from place to place. Generally, *belg* season showed the massive variability in rainfall amount and distributional patterns (24.7 – 55.1%) than *Kiremt* (15.3 – 21.4%) and *bega* (21.9 - 51.0%) seasons. Among the districts, the highest (55.1%), and the lowest (15.3%) degree of CV was reported, in Meket, during the *belg* and *bega* seasons, respectively. One of the possible reasons for such variation within the same locality could be due to the erratic nature of rainfall distribution which raised the seasonal rainfall variability in each of the districts. This again makes the area susceptible to droughts at different times.

Table 3 Seasonal and annual trend analysis of CHIRPS rainfall in North Wollo (2000-2019)

Season	*Statistics*	*Station-based values (mm)*												
		Dbre zebet	***Estayish***	***Gosh Meda***	***Hara***	***Kobo***	***Kone***	***Kulmesk***	***Lalibela***	***Mersa***	***Muja***	***Woldiya***	***Robit***	***Zobel***
Bega	Mean	74.8	88.0	71.7	132.1	81.9	66.3	86.5	65.4	117.0	90.6	143.3	95.8	77.7
	Std.D.	33.3	36.3	24.2	47.9	26.0	28.7	27.1	21.9	43.1	34.4	51.0	33.4	27.3
	CV (%)	44.5	41.2	33.8	36.2	31.8	43.2	30.3	33.5	36.9	38.0	35.6	34.8	25.9
	Sen's slope	2.500	2.427	0.912	1.655	0.632	1.907	1.793	1.548	0.540	2.478	2.803	1.426	0.582
	(p-Value)	**0.025****	**0.041****	0.230	0.538	0.626	**0.056***	**0.056***	**0.025****	0.922	0.144	0.256	0.284	0.721
Belg	Mean	207.3	181.8	182.6	271.9	169.5	173.5	166.3	144.8	266.7	179.4	256.7	205.3	198.1
	Std.D.	114.2	49.3	53.0	82.5	43.6	47.2	42.0	35.8	69.3	48.4	82.4	56.6	51.2
	CV (%)	55.1	27.1	29.0	30.3	25.8	27.2	25.3	24.7	29.7	27.0	32.1	27.6	35.2
	Sen's slope	5.0.5	3.286	4.354	5.131	2.304	3.668	2.435	1.641	4.231	2.438	4.715	3.200	2.172
	(p-Value)	0.127	0.127	**0.048****	0.122	0.230	**0.074***	0.163	0.256	0.315	0.230	**0.064***	0.144	0.417
Kiremt	Mean	744.6	723.1	628.8	669.1	440.3	737.3	611.7	638.9	559.8	645.7	600.3	500.2	432.3
	Std.D.	114.3	115.9	121.6	124.4	92.3	134.7	123.5	121.1	105.4	128.3	120.3	107.1	87.5
	CV (%)	15.3	20.2	19.3	18.6	21.0	18.3	20.2	19.0	18.8	19.9	20.0	21.4	20.2
	Sen's slope	0.188	0.279	-1.147	0.122	-3.184	-0.426	-3.072	-1.569	0.434	-0.719	2.094	-3.319	-3.854
	(p-Value)	1.000	1.000	0.922	1.000	0.496	0.974	0.538	0.770	0.974	0.974	0.871	0.581	0.256
Annual	Mean	1026.7	992.9	883.0	1073.0	691.7	977.2	864.5	849.0	943.4	915.8	1000.2	801.2	708.1
	Std.D.	110.9	158.6	138.6	142.3	100.8	144.8	128.9	120.6	125.6	130.8	149.0	109.4	104.1
	CV (%)	10.8	16.0	15.7	13.3	14.6	14.8	14.9	14.2	13.3	14.3	14.9	13.7	14.7
	Sen's slope	9.033	6.729	4.599	7.717	-1.418	6.226	1.540	1.203	5.021	4.293	10.702	0.239	-2.812
	(p-Value)	**0.012****	0.144	0.315	0.206	0.721	0.417	0.626	0.673	0.230	0.284	0.127	1.000	0.626

*, ** = statistically significant at $P < 0.1$ and 0.05, respectively

The Mann–Kendall test result indicated that an increasing trend of total annual rainfall has been observed in the majority of the stations with the highest significant trend (9.033 mm at p< 0.012) in Dbre zebit station of Meket district. However, Kobo and Zobel stations of the *kolla* agro-ecology showed a non-significant decreasing trend by -1.418 and -2.812, respectively. Though not significant, *kiremt* season was characterized by a decreasing trend of rainfall (-0.426 to -3.854 mm year^{-1}) in the majority of the stations. In contrast, stations like Debre zebet, Hara, Estayish, and Woldiya show an increasing trend, where the highest increase was observed in Woldia (2.094 mm year^{-1}). Studies conducted in different parts of Ethiopia by Suryabhagavan (2017), and Viste et al. (2012) reported similar statistically non-significant decreasing trend results of the *kremt* rainfall. Different from many parts of Ethiopia, the *belg* (2.03 – 0.54 mm year^{-1}), and *bega* (0.05 – 0.23 mm year^{-1}) seasons in the study area showed a very small increasing trend that was significant for some of the stations. In the study area, the decreasing trend of rainfall in *kiremt* and increasing during *bega* and *belg* has its own impact on *meher* season crop production in the area which, in turn, increase farmers' vulnerability to the upcoming droughts.

3.2. Drought assessment based on Z-Score index

The result of the 4-Month statistical Z-score (Fig. 4) showed temporal dry and wet years that occurred in North Wollo within the period (2000 – 2019). The figure provides a visual confirmation that the consecutive periods 2000

– 2001, 2016 – 2018, and the years 2007, 2010, and 2012 do not show rainfall deficit; of these, 2001, 2010, and 2016 were found to be the wettest years relative to the others. In those years a Z-score intensity of 0.32 – 2.15 has been observed indicating a moderately wet condition in the majority of the districts and very wet in few parts.

On the contrary, seven of the 20 years (2002, 2004, 2009, 2011, 2014, 2015, and 2019) were characterized by a rainfall deficit with a negative ZSI value. Though the spatial extent of affected areas and intensity level varies, there has been drought incidence in North Wollo each year. Among them, moderate drought had occurred in 2002 (Eastern part Kobo and Habru districts), 2004 (southwestern part of the Zone), and 2011 (in the entire Zone except for some western and Northern periphery). The years 2009 and 2015 were categorized as the driest years explained by severe to extreme drought conditions. In 2009, the western part of the Zone was affected by severe drought, whereas the central part extending from North to South was affected by moderate drought with a drought intensity ranging from -2.01 to -0.52. The highest Z-score intensities (-2.55) were also reported in the northern, central, and eastern parts of the basin. In this drought year, about 34.7, 47.2, and 17.9% of the area was affected by severe, moderate, and mild drought severity levels.

In the entire study period, a maximum range of Z-score intensities was detected in the year 2015 (-1.99 to -2.84), where 58.6% of the area was characterized by extremely severe drought conditions, and about 28.5 and 12.5% of the area was affected by severe and moderate droughts. Different studies and reports made assured that the year 2015 was a severe drought year in the Northern, Southern and Eastern parts of Ethiopia which caused successive harvest failures (50 – 90%) and widespread livestock deaths. This worst drought in half a century, triggered by the El Niño climatic phenomenon, left 10.2 million people in need of humanitarian assistance (Desportes 2016; Mohammed et al. 2017; Mekonen et al. 2020).

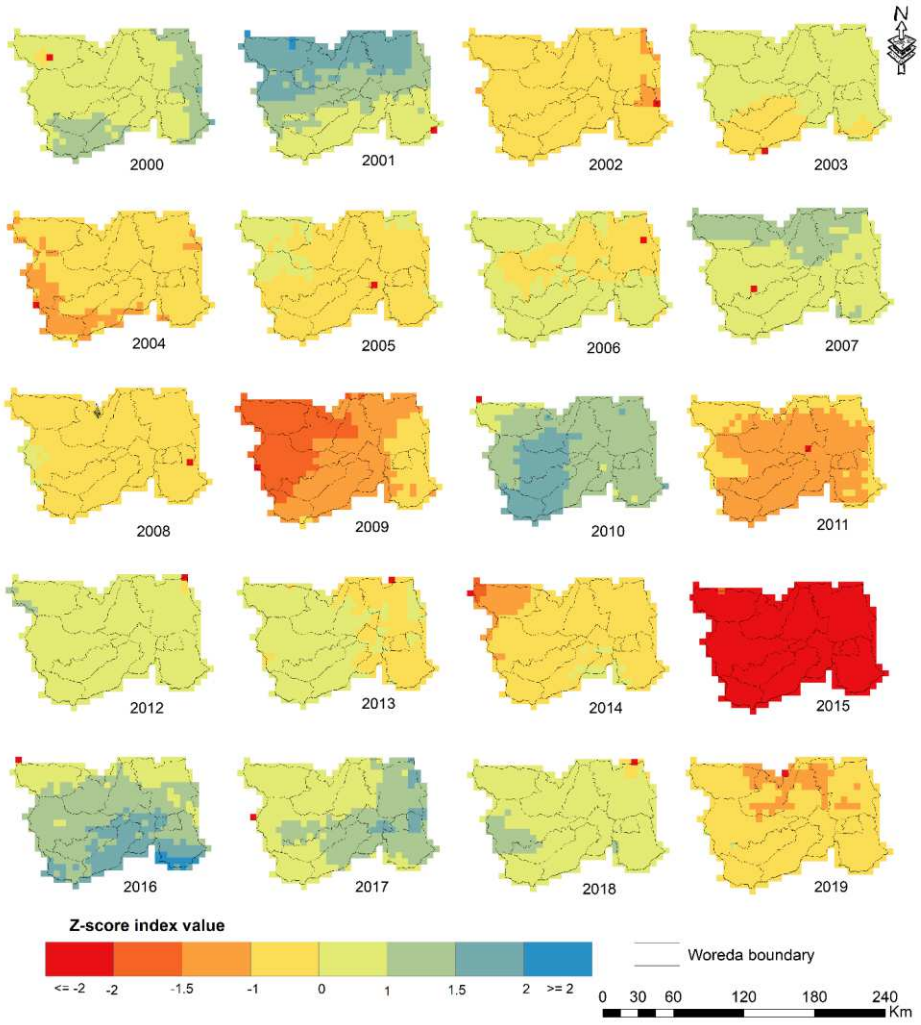

Fig. 4 Spatial and temporal distribution of meteorological drought based on a 4-monthly ZSI. The blue colors show non-drought seasons, whereas, the green, orange and red colors show drought seasons of the years.

Using the fifteen meteorological stations, clusters of stations were identified based on the highest correlation coefficient with each other depending on the similarity of rainfall patterns at each station. For stations showing similar pattern, three clusters; r = 0.98 – 0.99 (a), r = 0.97 – 0.98 (c), and r = 0.79 – 0.88 (b) were produced to extract the ZSI from the raster dataset (Fig. 5). Then, time series plots of meteorological drought intensities in each cluster of stations were plotted to prepare a clustered column chart (Fig. 5). The figure indicates the wet and drought years in most of the stations clustered together disregarding station locations. Therefore, the metrological drought intensity difference is clearly shown in the years 2002, 2004, 2009, 2011, 2014, 2015, and 2019. Similarly, the wet years in each cluster (2001, 2007, 2010, 2012, 2016, 2017, and 2018) were also clearly existing in the time series plot for almost all the stations.

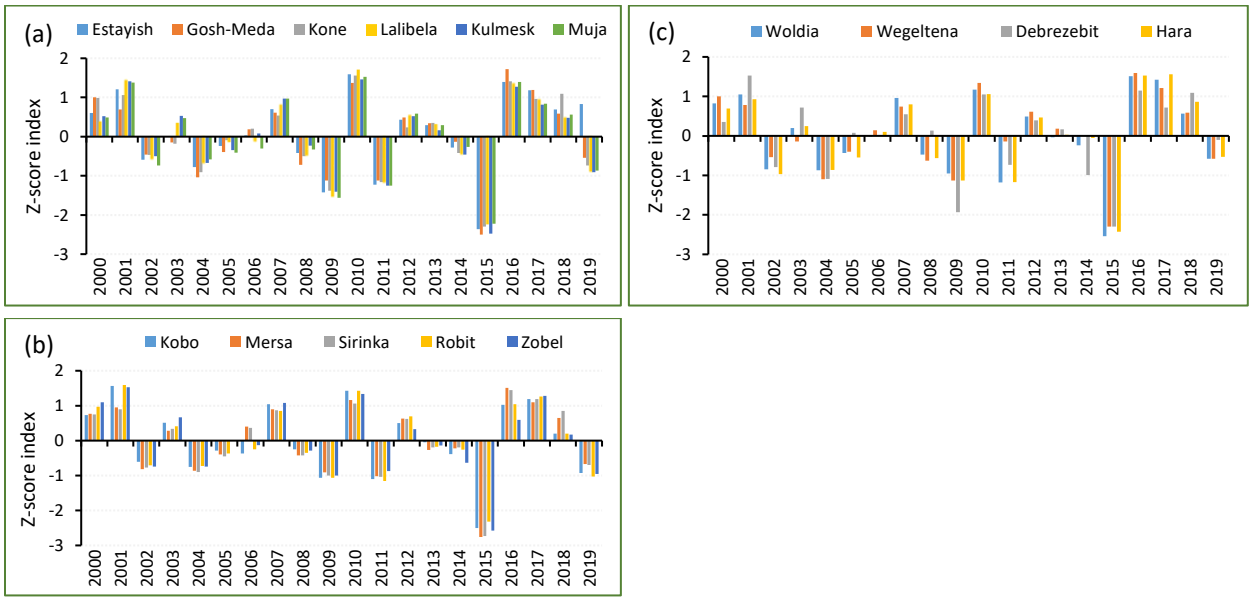

Fig. 5 Temporal pattern of the ZSI (2000 - 2019) in a clustered meteorological stations for the Kiremt season (June to September)

Similar study outputs were also obtained by Gebrehiwot et al. (2016) that country-wide drought conditions have been observed in the crop growing periods of 2000, 2002, 2009, and 2010 in the central and northern highlands of Ethiopia by using VCI as a drought indicator. Senamaw et al. (2021) also reported that the year 2009 and 2015 were the severe drought years in the Waghemra zone, the neighboring zone of the study area, over the period 2000 – 2016. Furthermore, they also noted that the years 2001 and 2007 were identified as wet years showing good crop yield. The United Nations Office for the Coordination of Humanitarian Affairs (UNOCHA) on its report emphasized the prevalence of two consecutive failed rainy seasons (2010 – 2011) in the dry lands of Ethiopia (including the study area), Somalia and Kenya, and considered it as one of the driest years since 1950/51 (www.unocha.org). This extreme lack of rain resulted drought and has reduced the ability of people to grow their food.

3.7. Relationship and trend analysis of ZSI and other climate variables

In drought analysis, it is quite useful to grasp the spatial and temporal trend of DIs and associated climate variables in an area. For such purposes, four stations (Kobo, Lalibela, Kone, and Estayish) were selected fairly representing *Kolla, Woina-dga, Dga*, and *Wurich* agro-ecologies, respectively. From these representative stations of the area, point-based values could feasibly be extracted, and examining the spatiotemporal trend of seasonal precipitation (PPt), ZSI, LST, and their anomalies was made possible.

Table 4 Pearson correlation matrix between the precipitation, NDVI and LST anomalies, and the ZSI, North Wollo (2000 - 2019)

Station Name		Index		Anomaly		Station Name		Index		Anomaly	
		ZSI	LST	PPt	LST			ZSI	LST	PPt	LST
Kobo	ZSI	1				Mersa	ZSI	1			
	LST	-0.442	1				LST	-0.49	1		
	PPt anomaly	-0.937	-0.38	1			PPt anomaly	0.977	-0.52	1	
	LST anomaly	-0.695	1.00	-0.682	1		LST anomaly	-0.489	1.00	-0.521	1
Lalibela	ZSI	1				Woldiya	ZSI	1			
	LST	-0.24	1				LST	-0.43	1		
	PPt anomaly	0.999	-0.25	1			PPt anomaly	0.986	-0.44	1	
	LST anomaly	-0.234	1.00	-0.245	1		LST anomaly	-0.427	1.00	-0.443	1
Debre zbet	ZSI	1				Kone	ZSI	1			
	LST	-0.39	1				LST	-0.11	1		
	PPt anomaly	0.991	-0.42	1			PPt anomaly	0.998	-0.100	1	
	LST anomaly	-0.392	1.00	-0.421	1		LST anomaly	-0.109	1.00	-0.100	1
Estayish	ZSI	1									
	LST	-0.44	1								
	PPt anomaly	0.937	-0.38	1							
	LST anomaly	-0.442	1.00	-0.376	1						

In all agro-ecologies (Fig. 6 and Table 4, 5) precipitation has shown a direct influence on ZSI, LST, and their anomalies. A strong positive significant relationship (r = 0.93 - 0.99) was observed with ZSI, and negative with LST (r = -0.1 to -0.52). Due to this, when precipitation deviates towards the positive (increase in amount as compared with the long-term mean value) ZSI also increases and vice versa. This makes clear that an increase in water availability results in an upward trend for ZSI and reduced drought incidents in the area. Therefore, ZSI shows a statistically significant increasing trend (R^2/P/α=1.00/<0.066/0.001 to 0.94/0.048/0.001) in all the stations. As expected, LST and its anomalies show a decreasing trend by -0.03 to -0.17% deviation from its long-term mean with a one percent rise of precipitation from its long-term mean value, and this was statistically significant (R^2/P/α=0.2/<0.050/0.05 to 0.31/0.012/0.05) in stations such as Goshmeda, Mersa, Muja, Robit, and Zobel.

Table 5 Station-based seasonal trend between ZSI, and related hydro-meteorological variables and their anomalies

X_i	Y_i	*Statistics*	*Debre zebet*	*Estayish*	*Gosh Meda*	*Hara*	*Kobo*	*Kone*	*Kulmesk*	*Lalibela*	*Mersa*	*Muja*	*Woldiya*	*Robit*	*Zobel*
PPt anomaly	LST anomaly	Trend	-0.173	-0.124	-0.168	-0.137	-0.124	-0.03	-0.090	-0.062	-0.117	-0.123	-0.104	-0.093	-0.131
		R^2	0.18	0.14	0.29	0.17	0.14	0.01	0.15	0.06	0.27	0.24	0.20	0.20	0.31
		P	< 0.065	< 0.103	**0.015**	< 0.077	< 0.103	< 0.674	< 0.100	< 0.297	**< 0.018**	**< 0.028**	< 0.051	**< 0.050**	**< 0.012**
		α			0.05						0.05	0.05		0.05	0.05
	ZSI	Trend	0.066	0.048	0.052	0.054	0.048	0.056	0.051	0.054	0.053	0.052	0.050	0.047	0.051
		R^2	0.98	0.88	0.98	0.94	0.88	0.99	0.99	0.99	0.96	1.00	0.97	0.96	1.00
		P	**<0.0001**	**<0.0001**	**<0.0001**	**<0.0001**	**<0.0001**	**<0.0001**	**<0.0001**	**<0.0001**	**<0.0001**	**<0.0001**	**<0.0001**	**<0.0001**	**<0.0001**
		α	0.001	0.001	0.001	0.001	0.001	0.001	0.001	0.001	0.001	0.001	0.001	0.001	0.001
LST anomaly	ZSI	Trend	-0.392	-0.068	-0.091	-0.070	-0.068	-0.020	-0.089	-0.050	-0.119	-0.102	-0.093	-0.100	-0.118
		R^2	0.15	0.20	0.29	0.19	0.20	0.01	0.18	0.06	0.24	0.25	0.18	0.19	0.31
		P	0.088	0.051	**0.014**	0.058	0.051	0.647	0.067	0.321	**0.029**	**0.027**	0.060	0.056	**0.012**
		α			0.05						0.05	0.05			0.05

** X_i= independent variable Y_i= dependent variable, R^2 = goodness of fit, P= p-value at α (alpha) confidence level; the bold value is significant at the specified α level.*

The Pearson correlation coefficient also confirmed a negative association (r = -11 to -49) between LST and ZSI. The highest and lowest correlation coefficients were obtained in Mersa (*kolla* area) and Kone (*dga* area) stations, respectively. This is because temperature rise in the cool areas has little effect in causing droughts than the already hot areas which are largely susceptible to drought conditions with a minimum deviation of LST from its long-term mean values. As stated earlier, decreasing in ZSI values towards the negative is an indicator of drought prevalence in an area. So, ZSI showed a decreasing trend (-0.119 to -0.0.02) with a unit percent rise of LST from its long-term mean in all the areas (Fig. 6). This was also significant in the majority of stations (at R^2/p/α=0.24/<0.029/0.05 to 0.01/<0.647/0.05).

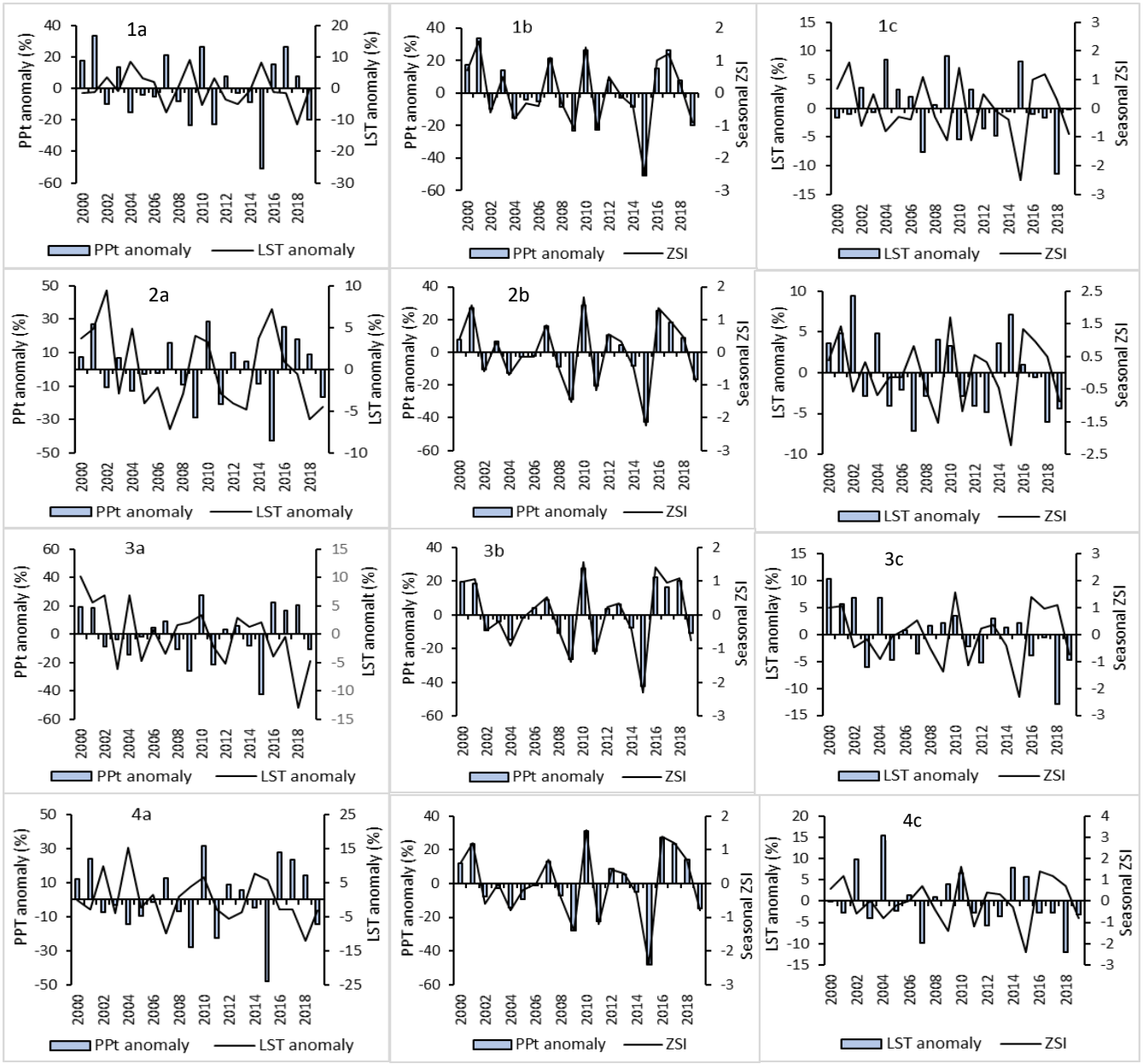

Fig. 6 Spatial and temporal trend of precipitation anomaly with the LST anomalies & ZSI, LST anomalies with the ZSI for 2000 to 2019. Warm semiarid (Kolla) area: 1a-1c, Kobo; Cool sub-humid (Woina-dga) area: 2a-2c, Lalibela; Cool humid (Dega): 3a-3c, Kone; Cold and moist (Wurich): 4a-4c, Estayish.

2.8. Classification of drought risk area

The frequency of drought for the study area was prepared by using the historical drought intensity map of ZSI (Fig. 7). The result confirmed the existence of multifaceted spatial variation in the frequency of drought episodes in the area. This shows that each district in the area was under rainfall deficit repeatedly for 15 and above times of the period. That is, mild to severe meteorological drought events knocked out the area about 15 – 18 times of the study period. As it was depicted from Figure 4, the majority of it (62.72%) was falling under mild drought (ZSI value of −

0.99 to 0.99) or abnormally dray conditions which usually showed only a slight variation from the normal rainfall (near normal) distribution. Even some drought studies like Desportes (2016), Mekonen et al. (2020), Mohammed et al. (2017) do not consider this range as a drought indicator. Such rainfall deficiency, however, has a great effect on vegetation growth, and thus, when triggered by high LST intensities, it usually propagates to agricultural droughts.

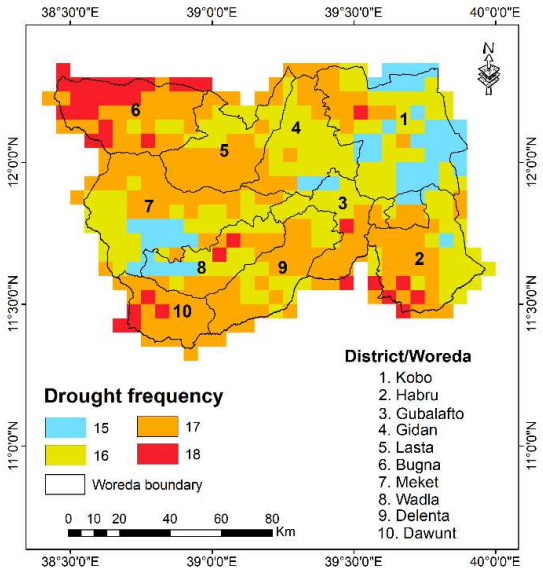

Fig. 7 Frequency of meteorological drought occurrence based on the ZSI, North Wollo (2000 - 2019).

In terms of area coverage, about 11.0, 35.6, 45.2, and 8.2% of the Zone experience a drought frequency of 15, 16, 17, and 18 times, respectively over the 20 years. As depicted from Fig. 7, the highest drought frequency was registered in Wadla, Habru, and Dlanta districts. Generally, based on such high drought frequency, we can conclude that the entire area of the zone falls under an extremely high drought risk level.

2.5. Conclusions

Drought is the most damaging natural hazard that occurs in both high and low rainfall areas and almost all climate regimes. Ethiopia has been continuously affected by recurrent droughts causing an immense impact on its economy, societal wellbeing, and environmental sustainability. The impacts were very serious in northeastern parts of Ethiopia, specifically, in places like North Wollo. As a result, early detection of droughts is necessary to monitor it effectively and reduce the impacts. The dataset used (CHIRPS monthly rainfall) was validated with the stations rainfall by applying statistical tests such as Pearson correlation, bias, ME, MAE, RMSE. The test results confirmed the good agreement between the two rainfall datasets. Hence, CHIRPS rainfall products could be used for drought detection and assessment in the study area, and data-scarce regions of Ethiopia in general.

Due to the erratic nature of rainfall distribution, the total annual rainfall revealed lower variability than each season. The study noted that *belg* season showed massive variability in rainfall amount and distributional patterns than *Kiremt* and *bega* seasons. An increasing trend of total annual rainfall has been observed in the majority of the districts (1.2 – 10.7 mm year^{-1}), whilst, *kiremt* season was characterized by a decreasing trend (-0.43 to -3.85 mm year^{-1}). However, the *belg* and *bega* seasons showed an increasing trend in most of the districts. A decreasing trend of rainfall in *kiremt* and increasing during *bega* and *belg* has its effect on *meher* season crop production, thereby, intensifying farmers' vulnerability to the upcoming droughts.

Based on the ZSI values, the wet and drought years over the period 2000 – 2019 were detected and characterized. Thus, 2001, 2010, and 2016 were identified as the wettest years with a Z-score intensity of 0.32 – 2.15. Nonetheless, 2009 and 2015 were categorized as the driest years elucidated by severe, and extreme drought conditions. As a result of the trend analysis among ZSI and associated climate variables, a decreasing trend (-0.12 to -0.02) of ZSI was observed with a unit percent rise of LST from its long-term mean. Hence, it is realized that the major factors that cause meteorological drought in the study area were the rising LST and erratic rainfall, which triggered a decrease in soil moisture, and less vegetation cover.

This study concluded that ZSI indicated the historic meteorological drought events of North Wollo within the study period reasonably well. In the ara, each district was under rainfall deficit repeatedly (15 – 18 times), so that it could be considered as an extremely high meteorological drought risk zone. The observed spatiotemporal meteorological drought risk events have shown a potential threat to the rainfed agricultural activities which impose immense influence on agro-based livelihoods of the local community. So, the study could give policymakers more information on regional and local drought monitoring and early warning systems, allowing them to improve existing monitoring, mitigation, and adaptation strategies designed to reduce the impacts of climate extremes and associated droughts. Finally, the study recommended further study on meteorological, and agricultural drought conditions of the area using additional DIs that could take into account the temperature, evapotranspiration, and soil moisture contents of all the seasons.

Abbreviations

AVHRR: Advanced Very High-Resolution Radiometer; CHIRPS: Climate Hazards Group InfraRed Precipitation with Stations; CPC: Climate Prediction Center; CSA: Central Statistical Agency; CV: Coefficient of variation; DAI: Drought Area Index; EOS: Earth-observing system; GIS: Geographic Information Systems; GWP: Global Water

Partnership; LST: Land Surface Temperature; MAE: Mean absolute error; MCTK: MODIS conversion tool kit; ME: Mean error; MODIS: Moderate Resolution Imaging Spectroradiometer; NCDC: National Climatic Data Center; NMA: National Meteorological Agency; RAI: Rainfall Anomaly Index; PDSI: Palmer Drought Severity Index; PN: Percent of Normal; RMSE: Root Mean Square Error; SPI: Standardized Precipitation Index; SSA: Sub-Saharan Africa; WMO: World Meteorological Organization; ZSI: Z-Score Index.

Acknowledgments

We would like to thank the USGS earth explorer for freely downloading different MODIS images of the study watershed from http://earthexplorer.usgs.gov. We also acknowledge the US Geological Survey (USGS) and the Climate Hazards Group at the University of California for developing the CHIRPS rainfall estimate and allowing us to freely download it at https://data.chc.ucsb.edu/products/CHIRPS-2.0/africa_monthly/. We are grateful to the Ethiopian National Meteorological Service Agency for providing us the daily rainfall and temperature data of the study area.

Competing of interests

The authors declared that they have no competing interests.

Funding

Funding information is not applicable / No funding was received.

Author's Contribution

The first author collect data, analyzes it, and wrote the manuscript. The second and third authors gave technical support and conceptual advice with comments for improvement. All authors discussed the contents, method, and results of the manuscript. They also read, edit and approved it.

Availability of data

The datasets used during the current study are freely available on websites listed in the acknowledgment.

References

Achite M, Caloiero T, Wał A, Krakauer N (2021) Analysis of the Spatiotemporal Annual Rainfall Variability in the Wadi Cheliff Basin (Algeria) over the Period 1970 to 2018. Water 13(1477):1–9. https://doi.org/10.3390/w13111477

Adhikari U, Nejadhashemi AP, Woznicki SA (2015) Climate change and eastern Africa : a review of impact on major crops. Food Energy Secur 4(2):110–132. https://doi.org/10.1002/fes3.61

Ahmadalipour A (2017) Multi-Dimensional Drought Risk Assessment Based on Socio-Economic Vulnerabilities and Hydro-Climatological Factors. Portland State University

Aragie T, Genanu S (2017) Level and Determinants of Food Security in North Wollo Zone (Amhara Region – Ethiopia). 5(6):232–247. https://doi.org/10.12691/jfs-5-6-4

Ayalew D (2012) Variability of rainfall and its current trend in Amhara region, Ethiopia. Afr J Agric Reseearch 7(10):1475–1486. https://doi.org/10.5897/ajar11.698

Ayehu G, Tadesse T, Gessesse B, Dinku T (2018) Validation of new satellite rainfall products over the Upper Blue Nile Basin , Ethiopia. Atmospheric Meas Tech 11:1921–1936. https://doi.org/10.5194/amt-11-1921-2018

Azadi H, Keramati P, Taheri F, Rafiaani P, Teklemariam D, Gebrehiwotg G, Hosseininiah H, Passelb S, Lebaillyi P (2018) Agricultural land conversion: Reviewing drought impacts and coping strategies. Int J Disaster Risk Reduct 31(2018):184–195. https://doi.org/10.1016/j.ijdrr.2018.05.003

Baniya B, Tang Q, Xu X, Haile GG, Chhipi-shrestha G (2019) Spatial and Temporal Variation of Drought Based on Satellite Derived Vegetation Condition Index in Nepal from 1982–2015. Sensors 19(430). https://doi.org/10.3390/s19020430

Bayissa Y, Tadesse T, Demisse G, Shiferaw A (2017) Evaluation of Satellite-Based Rainfall Estimates and Application to Monitor Meteorological Drought for the Upper Blue Nile Basin, Ethiopia. Remote Sens 9(669):1–17. https://doi.org/10.3390/rs9070669

Bayissa Y, Tadesse T, Svoboda M, Wardlow B, Swigart J, Andel S (2018) Developing a satellite-based combined drought indicator to monitor agricultural drought : a case study for Ethiopia. GIScience Remote Sens 00(00):1–31. https://doi.org/10.1080/15481603.2018.1552508

Belay A, Demissie T, Recha JW, Oludhe C, Osano PM, Olaka LA, Solomon D, Berhane Z (2021) Analysis of Climate Variability and Trends in Southern Ethiopia. climate 9(96):1–17. https://doi.org/10.3390/cli9060096

Bentoa VA, Gouveiaa CM, DaCamaraa CC, Trigoa IF (2018) A climatological assessment of drought impact on vegetation health index. Agric For Meteorol 259:286–295. https://doi.org/10.1016/j.agrformet.2018.05.014

Bewket W (2009) Rainfall variability and crop production in Ethiopia Case study in the Amhara region. In: Proceedings of the 16th International Conference of Ethiopian Studies. pp 823–836

Bhalme HN, Mooley DA (1980) Large-Scale Droughts/Floods and Monsoon Circulation. Indian Inst Trop Meteorol. https://doi.org/0027-0644/80/081197-15$07.75

Blain GC (2013) The Mann-Kendall test: the need to consider the interaction between serial correlation and trend. Acta Sci (iid):393–402. https://doi.org/10.4025/actasciagron.v35i4.16006

Cai G, Du M, Liu Y (2011) Regional Drought Monitoring and Analyzing Using MODIS Data — A Case Study in Yunnan Province. In: D. Li, Y. Liu and YC (ed) CCTA 2010, Part II, Internatio. pp 243–251

Camberlin P, Barraud G, Bigot S, Dewitte O, Makanzu IF, Maki Mateso JC, Martiny N, Monsieurs E, Moron V, Pellarin T, Philippon N, Sahani M, Samba G (2019) Evaluation of remotely sensed rainfall products over Central Africa. Q J R Meteorol Soc 145(722):2115–2138. https://doi.org/10.1002/qj.3547

CSA (2013) Population Projection of Ethiopia for all Regions from 2014 – 2017. CSA, Addis Ababa, Eethiopia

Dai A (2011) Drought under global warming: a review. WIREs Clim Change 2(1):45–65. https://doi.org/10.1002/wcc.81

Desportes I (2016) Responding to the 2016 drought amid political protest and a state of emergency in Ethiopia. Hague Netherland

Dinku T, Funk C, Peterson P, Maidment R, Tadesse T, Gadain H, Ceccato P (2018) Validation of the CHIRPS satellite rainfall estimates over eastern Africa. Adv Remote Sens Rainfall Snowfall (January):292–312. https://doi.org/10.1002/qj.3244

Dogan S, Berktay A, Singh VP (2012) Comparison of multi-monthly rainfall-based drought severity indices, with application to semi-arid Konya closed basin, Turkey. J Hydrol 470–471:255–268. https://doi.org/10.1016/j.jhydrol.2012.09.003

Dutra E, Magnusson L, Wetterhall F, Cloke H, Balsamo G, Pappenberger F (2013) The 2010 – 2011 drought in the Horn of Africa in ECMWF reanalysis and seasonal forecast products. Int J Climatol 33:1720–1729. https://doi.org/10.1002/joc.3545

Dutta D, Kundu A (2015) Assessment of agricultural drought in Rajasthan (India) using remote sensing derived Vegetation Condition Index (VCI) and Standardized Precipitation Index (SPI). Egypt J Remote Sens Space Sci 18(1):53–63. https://doi.org/10.1016/j.ejrs.2015.03.006

Ellis AW, Goodrich GB, Garfin GM (2010) A hydroclimatic index for examining patterns of drought in the Colorado River Basin. Int J Climatol 30(2):236–255. https://doi.org/10.1002/joc.1882

Eshetie M, Demisse B (2016) Evaluation of Vegetation Indices for Agricultural Drought Monitoring in East Amhara, Ethiopia. Int J Sci Res 5(10):535–540

Eze E, Girma A, Zenebe A, Zenebe G (2020) Feasible crop insurance indexes for drought risk management in Northern Ethiopia. Int J Disaster Risk Reduct 47:1–29. https://doi.org/10.1016/j.ijdrr.2020.101544

FAO (2015) The impact of disasters on agriculture and food security. Pakistan

Funk C, Peterson P, Landsfeld M, Pedreros D, Verdin J, Shukla S, Husak G, Rowland J, Harrison L, Hoell A, Michaelsen J (2015) The climate hazards infrared precipitation with stations — a new environmental record for monitoring extremes. Sci Data :1–21. https://doi.org/10.1038/sdata.2015.66

Gaikwad S, Kale K, Kulkarni S, Varpe AB, Pathare G (2015) Agricultural Drought Severity Assessment using Remotely Sensed Data : A Review. Int J Adv Remote Sens GIS 4(1):1195–1203

Gao F, Morisette JT, Wolfe RE, Ederer G, Pedelty J, Masuoka E, Myneni R, Tan B, Nightingale J (2008) An Algorithm to Produce Temporally and Spatially Continuous MODIS-LAI Time Series. 5(1):60–64

Gebre E, Berhan G, Lelago A (2017) Application of Remote Sensing and GIS to Characterize Agricultural Drought Conditions in North Wollo Zone , Amhara Regional State , Ethiopia. J Nat Sci Res 7(17)

Gebrechorkos S, Hülsmann S, Bernhofer C (2018) Evaluation of multiple climate data sources for managing environmental resources in East Africa. Hydrol Earth Syst Sci 22:4547–4564

Gebrehiwot T, Van der Veen A, Maathuis B (2016) Governing agricultural drought: Monitoring using the vegetation condition index. Ethiop J Environ Stud Manag 9(3):354. https://doi.org/10.4314/ejesm.v9i3.9

Gebrehiwot T, Veen A Van Der (2013) Climate change vulnerability in Ethiopia: disaggregation of Tigray Region. J East Afr Stud 7(4):607–629. https://doi.org/10.1080/17531055.2013.817162

Gebremicael TG, Mohamed YA, Zaag P Van Der, Amdom G (2017) Comparison and validation of eight satellite rainfall products over the rugged topography of Tekeze-Atbara Basin at different spatial and temporal scales. Hydrol Earth Systm Sci :1–31. https://doi.org/10.5194/hess-2017-504

Ghaleb F, Mario M, Sandra A (2015) Regional Landsat-Based Drought Monitoring from 1982 to 2014. climate 3:563–577. https://doi.org/10.3390/cli3030563

Gibbs W. J, Maher JV (1967) Rainfall Deciles as Drought Indicators. Bur. Meteorol. Bull. 48, Melbourne, Australia

Gocic M, Trajkovic S (2013) Analysis of changes in meteorological variables using Mann-Kendall and Sen's slope estimator statistical tests in Serbia. Glob Planet Change 100:172–182. https://doi.org/10.1016/j.gloplacha.2012.10.014

Gonfa L (1996) Climate Classification of Ethiopia. National Meteorological Service Agency (NMA), Ethiopia

Gray C, Mueller V (2012) Drought and Population Mobility in Rural Ethiopia. World Dev 40(1):134–145. https://doi.org/10.1016/j.worlddev.2011.05.023

Guo H, Bao A, Liu T, Jiapaer G, Ndayisaba F, Jiang L (2018) Spatial and temporal characteristics of droughts in Central Asia. Sci Total Environ 624:1523–1538. https://doi.org/10.1016/j.scitotenv.2017.12.120

Hailu S (2013) The Impact of Disaster Risk Management Interventions in Humanitarian Programmes on Household Food Security: The Case of East Africa, Ethiopia, Amhara Region, North Wollo Zone

Hare B (2003) Assessment of Knowledge on Impacts of Climate Change – Contribution to the Specification of Article 2 of the UNFCCC. Potsdam, Berlin 2003

Jain SK, Kumar V (2012) Trend analysis of rainfall and temperature data for India. Curr Sci 102(1):37–49

Jain VK, Pandey RP, Jain MK, Byun HR (2015) Comparison of drought indices for appraisal of drought characteristics in the Ken River Basin. Weather Clim Extrem 8:1–11. https://doi.org/10.1016/j.wace.2015.05.002

Kiem A, Johnson F, Westra S, Dijk A, Evans J, Donnell A, Rouillard A, Barr C, Tyler J, Thyer M, Jakob D, Woldemeskel F, Sivakumar B, Mehrotra R (2016) Natural hazards in Australia : droughts. Clim Change. https://doi.org/10.1007/s10584-016-1798-7

Kogan F, Guo W, Yang W (2019) Drought and food security prediction from NOAA new generation of operational satellites. Geomat Nat Hazards Risk 10(1):651–666. https://doi.org/10.1080/19475705.2018.1541257

Legesse G, Suryabhagavan K V (2014) Remote sensing and GIS-based agricultural drought assessment in East Shewa Zone, Ethiopia. Trop Ecol 55(3):349–363

Li F, Li H, Lu W, Zhang G, Kim JC (2019) Meteorological drought monitoring in Northeastern China using multiple indices. Water Switz 11(1):1–17. https://doi.org/10.3390/w11010072

Liou YA, Mulualem GM (2019) Spatio-temporal assessment of drought in Ethiopia and the impact of recent intense droughts. Remote Sens 11(15):1–19. https://doi.org/10.3390/rs11151828

Lyon B (2014) Seasonal Drought in the Greater Horn of Africa and Its Recent Increase during the March-May Long Rains. J Clim 27:7953–7975. https://doi.org/10.1175/JCLI-D-13-00459.1

Mahyou H, Karrou M, Mimouni J, Mrabet R, Mourid M El (2010) Drought risk assessment in pasture arid Morocco through remote sensing. Afr J Environ Sci Technol 4(12):845–852

McKee TB, Doesken NJ, Kleist J (1993) The Relationship of Drought Frequency and Duration to Time Scales. Eighth Conf Appl Climatol:17–22

Mekonen AA, Berlie AB (2020) Spatiotemporal variability and trends of rainfall and temperature in the Northeastern Highlands of Ethiopia. Model Earth Syst Environ 6(1):285–300. https://doi.org/10.1007/s40808-019-00678-9

Mekonen AA, Berlie AB, Ferede MB (2020) Spatial and temporal drought incidence analysis in the northeastern highlands of Ethiopia. Geoenvironmental Disasters 7(10). https://doi.org/10.1186/s40677-020-0146-4 (2020)

Mekonnen YA, Gokcekus H (2020) Causes and Effects of Drought in Northern Parts of Ethiopi. 12(3)

Mera GA (2018) Drought and its impacts in Ethiopia. Weather Clim Extrem 22:24–35. https://doi.org/10.1016/j.wace.2018.10.002

Mohammed Y, Yimer F, Tadesse M, Tesfaye K (2017) Meteorological drought assessment in northeast highlands of Ethiopia. Int J Clim Change Strateg Manag:1–20. https://doi.org/10.1108/IJCCSM-12-2016-0179

Morid S, Smakhtin V, Moghaddasi M (2006) Comparison of seven meteorological indices for drought monitoring in Iran. Int J Climatol 26(7):971–985. https://doi.org/10.1002/joc.1264

Mpelasoka F, Awange J, Zerihun A (2018) Science of the Total Environment Influence of coupled ocean-atmosphere phenomena on the Greater Horn of Africa droughts and their implications. Sci Total Environ 610–611:691–702. https://doi.org/10.1016/j.scitotenv.2017.08.109

Mpelasoka F, Hennessy K, Jones R, Bates B (2008) Comparison of suitable drought indices for climate change impacts assessment over Australia towards resource management. Int J Climatol 8:1283–1292. https://doi.org/10.1002/joc.1649

Munira S, Alves M, Marin M (2018) Evaluating Precipitation Estimates from Eta, TRMM and CHRIPS Data in the South-Southeast Region of Minas Gerais Site - Brazil. Remote Sens Artic 10. https://doi.org/10.3390/rs10020313

NMA (2007) Climate Change National Adaptation Programme of Action (NAPA) of Ethiopia. Addis Ababa

Palmer WC (1965) Meteorological Drought. Research Paper No. 45, Washington, DC

Patel NR, Choprab P, Dadhwal VK, Freer J (2007) Analyzing spatial patterns of meteorological drought using standardized precipitation index. Meteorol Appl 11:329–336. https://doi.org/10.1002/met.33

Rahman S, Jahan CS, Mazumder QH, Hosono T (2017) Drought Analysis and Its Implication in Sustainable Water Resource Management in Barind Area, Bangladesh. J Geol Soc India 89:47–56

Salehnia N, Alizadeh A, Sanaeinejad H (2017) Estimation of meteorological drought indices based on AgMERRA precipitation data and station-observed precipitation data. J Arid Land. https://doi.org/10.1007/s40333-017-0070-y

Senamaw A, Addisu S, Suryabhagavan K V (2021) Mapping the spatial and temporal variation of agricultural and meteorological drought using geospatial techniques, Ethiopia. Environ Syst Res 10(15). https://doi.org/10.1186/s40068-020-00204-2

Singh R, Cross R, Crescent R, Centre C (2017) Reality of Resilienc: 2016-17 drought in East Africa. Resil Intel

Sruthi S, Aslam MAM (2015) Agricultural Drought Analysis Using the NDVI and Land Surface Temperature Data; a Case Study of Raichur District. Aquat Procedia 4:1258–1264. https://doi.org/10.1016/j.aqpro.2015.02.164

Suryabhagavan K V. (2017) GIS-based climate variability and drought characterization in Ethiopia over three decades. Weather Clim Extrem 15:11–23. https://doi.org/10.1016/j.wace.2016.11.005

Thenkabail PS, Gamage MS, Smakhtin V (2004) The Use of Remote Sensing Data for Drought Assessment and Monitoring in Southwest Asia. Colombo, Sri Lanka

Tilahun K (2006) Analysis of rainfall climate and evapotranspiration in arid and semi-arid regions of Ethiopia using data over the last half a century. J Arid Environ 64:474–487. https://doi.org/10.1016/j.jaridenv.2005.06.013

Toté C, Patricio D, Boogaard H, Wijngaart R Van Der, Tarnavsky E, Funk C (2015) Evaluation of Satellite Rainfall Estimates for Drought and Flood Monitoring in Mozambique. Remote Sens 7:1758–1776. https://doi.org/10.3390/rs70201758

Trnka M, Hayes M, Jurečka F, Bartošová L, Anderson M, Brown J, Camarero JJ, Cudlín P, Dobrovolný P, Eitzinger J (2018) Priority questions in multidisciplinary drought research. Clim Res. https://doi.org/10.3354/cr01509

Van rooy MP (1965) A Rainfall Anomaly Index (RAI), Independent of the Time and Space. Notos 14:43–48

Verdin J, Klaver R (2002) Grid-cell-based crop water accounting for the famine early warning system. Hydrol Process 16:1617–1630. https://doi.org/10.1002/hyp.1025

Vicente-Serrano SM, Begueria S, Lo´ Pez-Moreno JI (2010) A Multiscalar Drought Index Sensitive to Global Warming: The Standardized Precipitation Evapotranspiration Index. J Clim 23:1696–1718. https://doi.org/10.1175/2009JCLI2909.1

Viste E, Korecha D, Sorteberg A (2012) Recent Drought and Precipitation Tendencies in Ethiopia. Theor Appl Climatol

Wang W, Chen X, Shi P, Van Gelder PHAJM (2008) Detecting changes in extreme precipitation and extreme streamflow in the Dongjiang River Basin in southern China. Hydrol Earth Syst Sci 12(1):207–221. https://doi.org/10.5194/hess-12-207-2008

Wassie SB (2020) Natural resource degradation tendencies in Ethiopia: a review. Environ Syst Res 9(1):1–29. https://doi.org/10.1186/s40068-020-00194-1

WMO, GWP (2016) Handbook of Drought Indicators and Indices, Drought Mi. DigitalCommons@University of Nebraska - Lincoln, Lincoln Drought

Wu D, Qu J, Hao X (2015) Agricultural drought monitoring using MODIS-based drought indices over the USA Corn Belt. Int J Remote Sens 36(21):5403–5425. https://doi.org/10.1080/01431161.2015.1093190

Wu H, Hayes MJ, Weiss A, Hu Q (2001) An evolution of the standardized precipitation index, the China-Z index and the statistical Z-score. Int J Climatol 21(6):745–758. https://doi.org/10.1002/joc.658

Yuan Z, Xu J, Chen J, Huo J, Yu Y, Locher P, Xu B (2017) Drought Assessment and Projection under Climate Change: A Case Study in the Middle and Lower Jinsha River Basin. Adv Meteorol 2017. https://doi.org/10.1155/2017/5757238

Zargar A, Sadiq R, Naser B, Khan FI (2011) A review of drought indices. Env Rev 19:333–349. https://doi.org/doi:10.1139/A11-013

Zhang J, Mu Q, Huang J (2016) Assessing the remotely sensed Drought Severity Index for agricultural drought monitoring and impact analysis in North China. Ecol Indic 63:296–309. https://doi.org/10.1016/j.ecolind.2015.11.062